

Collaboration Between UME and LNE-INM on Co–C Eutectic Fixed-Point Construction and Characterization

M. Sadli · O. Pehlivan · F. Bourson · A. Diril ·
K. Ozcan

Published online: 2 July 2008
© Springer Science+Business Media, LLC 2008

Abstract Metal-carbon eutectic fixed-point construction and characterization are subjects of ongoing investigation within the field of radiation thermometry. National metrology institutes are in constant search of stable eutectic points with minimal uncertainty for the purposes of either increasing the working temperature range of radiation thermometry or obtaining intermediate check points for both contact and non-contact thermometries. The Co–C eutectic point ($\sim 1,324^{\circ}\text{C}$) would be very effective in reducing certain calibration uncertainties at this temperature, once long-term stable and reproducible cells are constructed. For these purposes, one Co–C eutectic cell was fabricated at UME, in collaboration with LNE-INM, while a second Co–C cell was constructed for UME. At UME, the cell was filled (in the Vega-BB3500PG blackbody) using methods developed by LNE-INM. Eutectic plateaux, eutectic temperatures, and their uncertainties have been assessed using the UME Transfer Standard Pyrometer TSP-2, calibrated at UME, and an IKE LP3, calibrated at INM. The two Co–C eutectic cells (one constructed at INM and the other at UME) were compared at UME. The short-term stability and reproducibility of the cells have been assessed for various thermal conditions. A provisional uncertainty budget for the thermodynamic temperature of the Co–C cell as determined by LNE-INM has been established.

Keywords Cobalt–carbon eutectic · Metal-carbon eutectic fixedpoints · Radiation thermometry

M. Sadli (✉) · F. Bourson
Institut National de Métrologie, LNE-INM/Cnam, 61 rue du Landy–case I 361,
93210 Saint-Denis, La plaine, France
e-mail: mohamed.sadli@cnam.fr

O. Pehlivan · A. Diril · K. Ozcan
UME, National Metrology Institute of Turkey, Kocaeli, Turkey

1 Introduction

Metal-carbon eutectic fixed points have been under study for a number of years and the important progress accomplished to date allows the thermometry community to believe in a probable future utilization of these points in the International Temperature Scale [1–4], if not as new fixed points of a revised scale, then at least as one of the routes for the *Mise en pratique* for the definition of the kelvin (together with thermodynamic temperature measurements). LNE-INM has been involved in the European project HIMERT [5], and has constructed, characterized [6, 7], and compared a set of its cells to other national metrology institutes (NMI) realizations [8]. A collaboration was started with UME in order to share experiences in the field of high-temperature measurements and to provide UME with assistance for metal-carbon cell filling and implementation techniques. The two laboratories use the same kind of furnace and have agreed to long-term cooperation on the Co–C eutectic point ($\sim 1,324^\circ\text{C}$), which would be very effective in decreasing certain calibration uncertainties at this temperature, once long-term stable and reproducible cells are constructed. This will also be part of the international efforts devoted to the assessment of the capabilities of metal(carbide)-carbon eutectic points [9].

For these purposes, two Co–C cells were filled in the Vega HTBB 3200PG furnace at LNE-INM in the presence of UME researchers, and in the HTBB 3500PG at UME in the presence of an LNE-INM researcher, using the methods developed by LNE-INM. These two Co–C eutectic cells were then compared. The short-term stability and reproducibility of the cells have been assessed for various thermal conditions. The aim of this common work is to improve the filling technique, the design of the crucibles, and the thermal conditions for the study of the melt-freeze plateaux of this eutectic point. This project also aims to check the reproducibility of the cells and their suitability for assessing the equivalence of ITS-90 realizations by the two laboratories.

In Sect. 5, the latest developments to this end at LNE-INM are described. A new filling technique that seeks to minimize the risk of contamination of the cell by avoiding direct exposure of the metal-carbon mixture to the furnace heater is presented.

2 Construction of Cell at UME

The eutectic cell, UME-2, consisting of the crucible, cap, and inner sleeve parts, is constructed from R-550 type graphite. Details of the cell design and material specifications are summarized in Table 1. Additionally, a graphite funnel was constructed for the filling, which is done in an HTBB 3500PG furnace operated vertically. Before starting the filling procedure, all graphite pieces (crucible, extension, and cap) are baked in the HTBB at a temperature $\sim 200^\circ\text{C}$ above the Co–C eutectic temperature in order to reduce the risk of contamination from the burning of some of the chemical components that may have been introduced during the machining and cleaning processes.

Cobalt and graphite powders were mixed at $\sim 2.4\%$ C in Co (by mass), which is slightly below the eutectic composition (2.6%). For this purpose, 0.63 g of graphite powder and 25 g of cobalt powder were mixed and the crucible was filled with the

Table 1 Details of the Co–C cells constructed at LNE-INM and UME

	UME-1 cell (filled at LNE-INM)	UME-2 cell (filled at UME)
Crucible material	SGL 4550 graphite, Density: $1.84 \text{ g} \cdot \text{cm}^{-3}$	R-550 type graphite, Density: $1.83 \text{ g} \cdot \text{cm}^{-3}$
	30 ppm impurity content in ash	20 ppm impurity content in ash
Cobalt powder specs	Alfa-Aesar 99.998 % purity	
Graphite powder specs	Alfa-Aesar 99.9999 % purity	
Amount of cobalt	35 g	34.78 g
Dimensions of cells	Cavity diameter: 3 mm Cavity length: 30 mm Outer diameter: 25 mm Length: 40 mm	

mixture under an argon atmosphere. Filling of the cell was performed in four separate steps. During the first filling, about 11 g of hypo-eutectic Co–C mixture was put inside the cell with its extension and melted. In the second step, 12.5 g of the mixture was added. After the second filling, the surface of the solidified metal-carbon mixture was noticed to be darker than after the first step. For this reason, during the third filling, 4.8 g of pure cobalt and only 1.8 g of the mixture were added. During the fourth and last filling step, 5.2 g of pure metal was added and the cap of the cell was screwed to the crucible. After this, the cell was ready to be run horizontally in the HTBB.

Prior to the study of the new cell and its comparison with the Co–C cell constructed at LNE-INM (UME-1 cell), care was taken to improve the temperature uniformity of UME's HTBB 3500PG by making various ring resistance measurements and ordering the ring elements in such a way that the heat leakage is compensated to some extent (cf. Sect. 3.1).

3 Measurements

3.1 Ring-Resistance Measurements and Improvement of the Furnace Temperature Uniformity

BB3500/BB3200 furnaces use a stack of pyrolytic-graphite rings as the heater tube. A compression spring presses the back copper electrode onto the pyrolytic-graphite rings, which are then pressed against the front electrode. Surrounding the cavity is a graphite heat shield—a large graphite tube filled with graphite fabric. This allows operation up to 3,500/3,200 °C, respectively.

The axial temperature distribution can be optimized by ordering the ring elements based on their individual electrical resistivities measured at room temperature [10] such that the rings with the higher resistivities are situated near the ends of the heater tube. The setup used for measuring the ring resistance is shown in Fig. 1 and was inspired by what was done previously at VNIIOFI (the manufacturer of the furnace). In this setup, the ring resistivity is obtained by measuring the voltage between the upper and the lower cylindrical electrodes, made of brass, enclosing the ring, at a 10 A

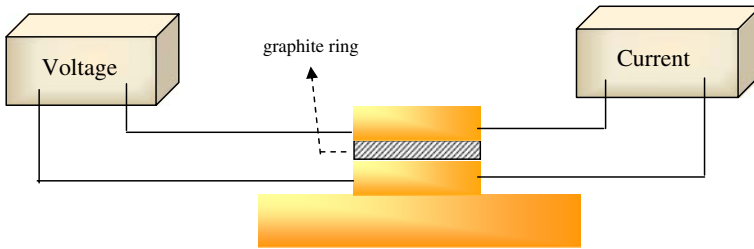


Fig. 1 Ring resistance measurement setup

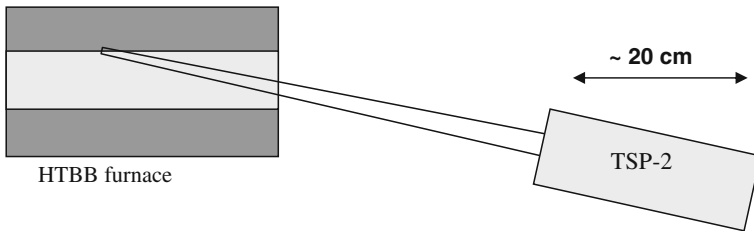


Fig. 2 Furnace uniformity measurement setup

bias current. After the measurements, the rings were numbered according to their positions in the furnace.

After the rings were positioned in the furnace, a temperature-uniformity measurement was performed. During this measurement, a TSP-2 was used as the thermometer; the cell holder was taken out of the furnace, and an additional cylinder was inserted into the furnace in place of the cell holder. Initially, the TSP-2 was focused on the middle of the furnace. Then, the focal point was scanned along the furnace wall by offsetting the viewing angle by 5° . This is represented schematically in Fig. 2, in which the rectangular block on the left represents the furnace, and the cylinder on the right represents the TSP-2 thermometer. The results of the uniformity measurements for the UME HTBB are given in Fig. 3. In order to obtain good temperature uniformity along the Co–C cell cavity, the cell is placed within the most uniform region of the furnace.

3.2 Influence of the Furnace-Parameter Settings

In order to investigate the dependence of the apparent eutectic temperature on the furnace parameters (the stabilization temperatures before initiating the plateaux, the increase in current, and the rate of change of current), the following procedure was put into practice. The furnace is heated and stabilized to a temperature a certain amount (ΔT) lower (or higher, for freezing) than the eutectic temperature. Melting (or freezing) is initiated with an increase (decrease) of current, ΔI , at a specific rate of change of current, R . The dependence of the eutectic melting temperature, determined as *the inflection point* of the melting curve, on these three furnace heating parameters, ΔT , ΔI , and R , has been investigated.

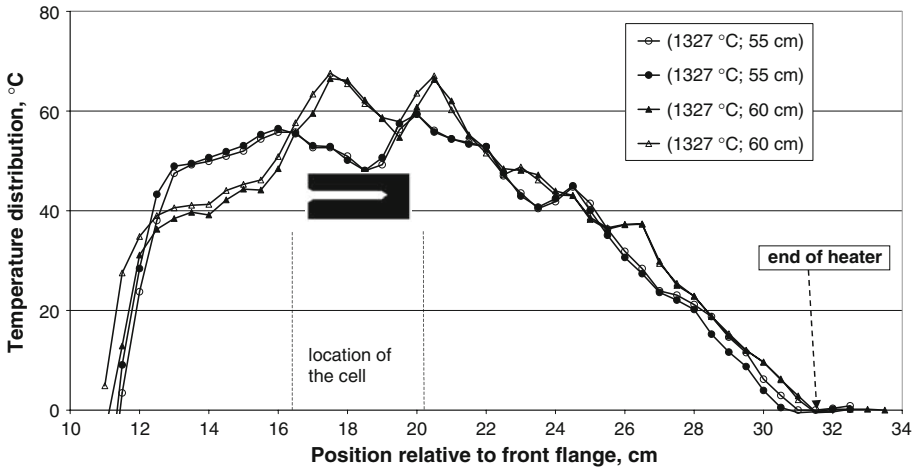


Fig. 3 Furnace uniformity measurements at two different working distances

For the melting temperature, no significant dependence on ΔT , ΔI , or R was observed. However, the freezing plateau is unsatisfactory when the cooling rate is less than $5 \text{ A} \cdot \text{min}^{-1}$ (which is around $20^\circ\text{C} \cdot \text{min}^{-1}$) or ΔT is less than 10°C . This is most probably due to the temperature uniformity of the furnace being insufficient to allow small rates of change and small temperature differences.

3.3 Eutectic-Temperature Measurement: Comparison of Results Obtained at UME and INM for the Same Cell, UME-1

The UME-1 cell (constructed at LNE-INM by UME staff) was studied at LNE-INM and at UME in order to check if their ITS-90 realizations are equivalent at this temperature within the combined uncertainties achievable at these laboratories.

For the measurement of the eutectic temperature, UME utilized the Vega TSP-2 pyrometer together with the Vega HTBB 3500PG furnace. The TSP-2 works in the temperature range of 800°C to $2,500^\circ\text{C}$ with a 650 nm optical head (Si-S1337-66BQ Hamamatsu photodiode). The minimum spot size is $0.6 \text{ mm} \times 0.8 \text{ mm}$ at 400 mm focal length. It is equipped with a shutter located near the field aperture for dark-current measurements. A Peltier cooler ensures that the detector and filter temperature stabilization is better than $\pm 0.1^\circ\text{C}$. Calibration of the TSP-2 is performed at the copper fixed point according to the requirements of the ITS-90. Spectral responsivity, non-linearity, and size-of-source effect (SSE) measurements are made using UME laboratory facilities.

LNE-INM used a Vega HTBB 3200PG furnace to study the cell in question. The pyrometer used for the measurements is an IKE LP3 operating at a wavelength of 650 nm and characterized for spectral responsivity, non-linearity, SSE, and calibrated at the Cu point.

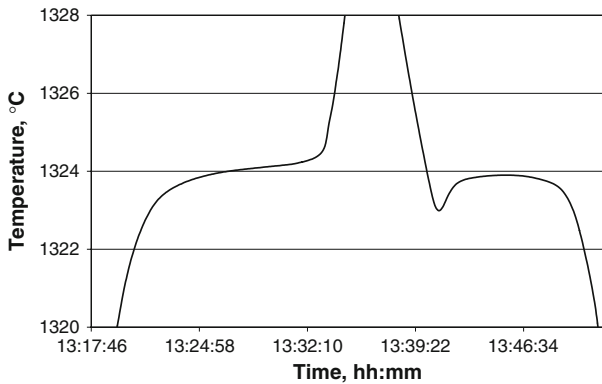


Fig. 4 Melting and freezing plateaux of the UME-1 cell measured at UME

Table 2 Melting temperatures and uncertainties obtained at LNE-INM and UME

Co–C Cell	$t_{\text{LNE-INM}}$ (°C)	t_{UME} (°C)	Difference (°C)	U_{LNE} (°C) $k = 2$	U_{UME} (°C) $k = 2$	Combined uncertainty (°C)
UME1	1,323.85	1,323.97	0.12	0.25	0.2	0.35
UME2	n/a	1,323.96	n/a	n/a	0.2	n/a

Typical melting and freezing curves obtained at UME are shown in Fig. 4. The melting temperature of the Co–C eutectic cell at LNE-INM is determined by inflection-point analysis [7]. At UME, the melting point is assessed by considering the standard deviation of a certain number of pyrometer readings during plateau realization, and taking the average signal in the range where the standard deviation is a minimum and where the signal is relatively constant. No significant difference was observed between the inflection-point method and the standard deviation method.

The melting temperature determined for this cell at LNE-INM was 1,323.85 °C with an uncertainty of 0.25 °C ($k = 2$). The same cell, measured a few months later at UME, showed a melting temperature of 1,323.97 °C with an uncertainty of 0.2 °C ($k = 2$) (Cf. Table 2, row 2). The full uncertainty budget associated with realization of the Co–C eutectic fixed point at LNE-INM and UME is given in Table 3.

The difference in melting temperatures measured at the two laboratories (120 mK) is within the combined uncertainties (320 mK).

3.4 Comparison of the Cells UME-1 and UME-2

The melting temperatures of the two Co–C cells UME-1 (constructed at LNE-INM by UME staff) and UME-2 (constructed at UME) were compared at UME. The two cells were studied within 2 days; the TSP-2 is considered as being stable during this period. Results of melting plateau measurements for UME-1 and UME-2 are given in column 2 of Table 2, and the associated uncertainties are given in row 2 of Table 2. The

Table 3 Uncertainty budget for the melting-temperature determination

Component	Description	LNE-INM ($k = 1$) (mK)	UME ($k = 1$) (mK)
ITS-90 temperature determination	Accounting for the temperature reference and the pyrometer functions	115	90
Repeatability	Repeatability of inflection point on the same day with the same furnace settings	10	10
Reproducibility	Plateaux for different furnace conditions (different temperature distributions and temperature steps)	45	40
Emissivity	Calculated as $0.9997 \pm 5 \times 10^{-5}$	6	6
Combined uncertainty ($k = 1$)		125	100

full uncertainty budget for realization of the Co–C eutectic fixed point at LNE-INM and UME is given in Table 3.

The cells have proven remarkably repeatable in the HTBB, although the temperature uniformity was not considered to be good. The repeatability of the inflection point during the melt plateau for the two cells over a series of five to six plateaux was, for each cell, better than 10 mK. The difference between the melting temperatures of the two cells was 10 mK. This difference is therefore not significant, and the cells can be considered equivalent even though the filling conditions were different and different crucibles were used (different graphite, different machining and cleaning conditions). The cobalt originated from the same company, although not from the same lot number.

Unfortunately, cell UME-2 was broken during these measurements. The crack inside the cavity expanded and the cavity was cut into two parts. Moreover, the cap was broken at the same position as the first cap. Figure 5 shows the last melt-freeze cycle performed with this cell.

The high-density graphite used may be the cause of these breakages. The brittleness of high-density graphite has also been observed at LNE-INM where many cells were broken recently. In the future, a compromise should be found between the density and the thermal expansion of the graphite.

4 New Filling Technique

At LNE-INM, the improvement of the metal-carbon eutectic cells, in terms of construction and implementation, is an ongoing task. An important effort was devoted in recent months to the Co–C eutectic point. The filling technique and the design of the cell have been revised. The aim of these new developments is to fill our Co–C cells in one filling step in order to:

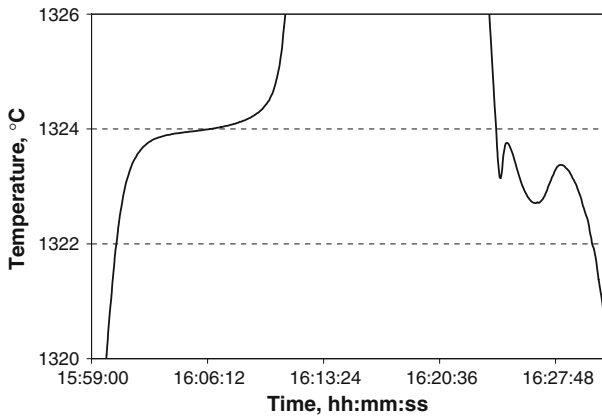


Fig. 5 Last melting and freezing plateaux for UME2 Co-C cell before breakage (during the freeze)

- Reduce the risk of contamination by total confinement of the metal-carbon mixture. Moreover, the fact that only one melt is necessary for complete filling of the cell reduces the risk of contamination.
- Fill the cells completely.
- Have good control of the furnace temperature during the filling. The piston moves down when the eutectic melts. This shows that the furnace has reached the eutectic melting temperature and helps avoiding overheating.
- Prepare a sample of the eutectic mixture for analysis. A sample of the MC eutectic is obtained after the melt (stays inside the piston).

This method has been successfully implemented for several cells. However, the large expansion coefficient of the cobalt was probably the cause of several breakages of the cells during the study.

Figure 6 shows the details of the fourth generation of cells and the filling setup. The metal and graphite mixture is introduced inside the cell and the extension. The piston is introduced inside the extension and comes in contact with the mixture (slightly below the eutectic composition). The piston is equipped with a graphite rod long enough to emerge from the furnace. The rod is used to push on the piston when the melt starts. During the melt, the excess metal-carbon is introduced inside the piston inner funnel through a 2 mm diameter hole. This is the sample dedicated to impurity analysis, which allows us to take into account possible contamination from the filling process. The piston is pulled by a few millimeters before the freeze starts in order to avoid sticking of the metal-carbon mixture to the graphite of the piston. When the cell reaches room temperature, it is extracted from the HTBB and the extension is removed and replaced by the cap. The cell is then ready to be run.

One major change to our cells is the usage of C/C sheets inside the crucible in order to increase the temperature uniformity around the metal-carbon ingot. This has proven to be efficient [10], and we have noticed improvement in the quality of the plateaux, as can be seen in Fig. 7. Improving the temperature uniformity of the HTBB 3200 furnace [11, 12] has also improved the quality of the plateaux.

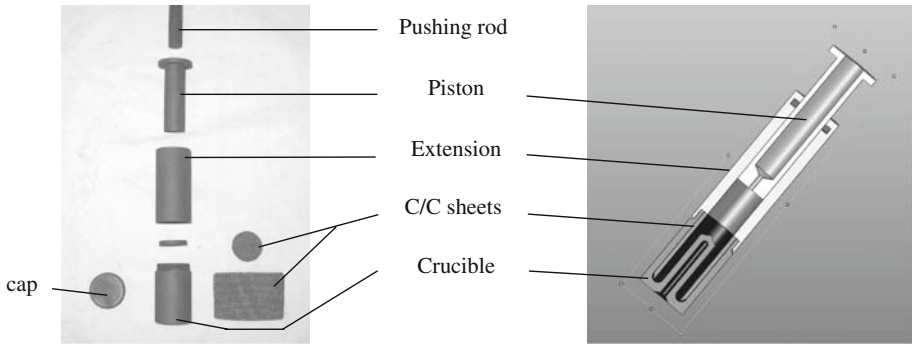


Fig. 6 New design of LNE-INM cells, involving CC sheets. On the right, a schematic of the assembly of the cell-funnel-piston system for a one-step filling successfully tested for the Co–C point

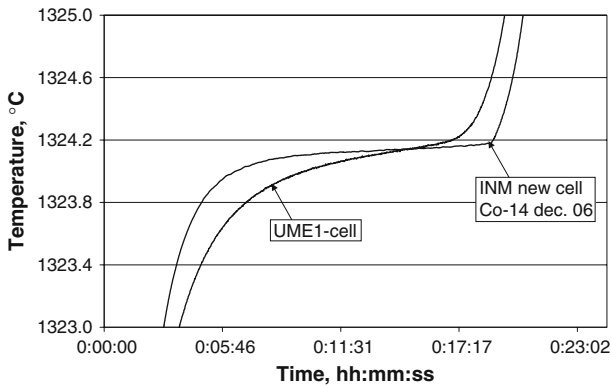


Fig. 7 Improvement of the melting plateau of LNE-INM cells with the evolving design and filling technique

5 Conclusions and Prospects

Two Co–C cells filled under different conditions by different persons, but with cobalt provided by the same company (although not the same lot), appear to be equivalent within the 10 mK repeatability of the plateaux.

Melting temperatures obtained with the same cell in both laboratories (UME and LNE-INM) agree within 120 mK, with an uncertainty in the difference of 320 mK. However, the plateau shape and temperature were found to be strongly dependent on the location of the cell within the furnace, showing that the furnace temperature uniformity should be assessed prior to using the cells.

Besides furnace characterization, future work will focus on the determination of the thermodynamic temperatures of eutectic fixed points. At LNE-INM, the measurement of the thermodynamic temperature of the metal (carbide)-carbon eutectic fixed points is one of the major research topics. An LP3 pyrometer has been equipped with additional filters, especially one at 850 nm, and a facility based on a tuneable Ti:sapphire laser is being set up to determine the absolute spectral responsivity of the pyrometer.

Table 4 Provisional uncertainty budget for thermodynamic temperature measurement at LNE-INM for a temperature of 2,000 K and a wavelength of 850 nm

	Relative uncertainty, $10^{-4}\sigma(X)/X$	$\sigma(T)$ (mK)
Source homogeneity	5	100
Source stability	0.5	10
Aperture area measurement ^a	7	140
Distance between source and detector ^a	5	100
Detector calibration ^b	10 \Rightarrow 4	200 \Rightarrow 80
Radiance meter inter-reflections	2	40
SSE	1	20
Emissivity	2	40
Combined uncertainty ($k = 1$)		260 \Rightarrow 180

^a These two calibrations can be improved by in-house methods

^b Traceability to the cryogenic radiometer can be made more straightforward with a lower uncertainty

The principle of this work has already been applied to the thermodynamic temperature measurement of the copper fixed point [13].

At a wavelength of 850 nm and for a temperature of 2,000 K, the standard uncertainty of the thermodynamic temperature that can be achieved with the present state of the art at LNE-INM is about 0.26 K. With a more direct traceability of the trap detector to the cryogenic radiometer, the standard uncertainty should soon fall to 0.18 K, and hopefully to a lower value in the near future. The uncertainty budget for thermodynamic temperature measurement at LNE-INM is given in Table 4.

At UME, we expect to start working with filter radiometers developed by the radiometry group and to use them for thermodynamic temperature measurements at the highest temperatures. It will be very useful to compare these methods in the future because they are based on different principles: imaging, or radiance mode, at LNE-INM and irradiance mode at UME.

References

1. Y. Yamada, H. Sakate, F. Sakuma, A. Ono, in *Proceedings of TEMPMEKO '99, 7th International Symposium on Temperature and Thermal Measurements in Industry and Science*, ed. by J. F. Dubbeldam, M.J. de Groot (Edauw Johannissen BV, Delft, 1999), pp. 535–540
2. Y. Yamada, MAPAN–J. Metrol. Soc. India **20**, 183 (2005)
3. E.R. Woolliams, G. Machin, D.H. Lowe, R. Winkler, *Metrologia* **43**, R11 (2006)
4. M. Sadli, J. Fischer, Y. Yamada, V.I. Sapritsky, D.H. Lowe, G. Machin, in *Proceedings of TEMPMEKO 2004, 9th International Symposium on Temperature and Thermal Measurements in Industry and Science*, ed. by D. Zvizdic (FSB/LPM, Zagreb, Croatia, 2004), pp. 341–347
5. G. Machin, G. Beynon, F. Edler, S. Fourrez, J. Hartmann, D. Lowe, R. Morice, M. Sadli, M. Villamañan, in *Temperature: Its Measurement and Control in Science and Industry*, vol. 7, ed. by D.C. Ripple. AIP Conference Proceedings, 684 (AIP, Melville, New York, 2003), pp. 285–290
6. M. Sadli, M. Fanjeaux, G. Bonnier, in *Temperature: Its Measurement and Control in Science and Industry*, vol. 7, ed. by D.C. Ripple. AIP Conference Proceedings, 684 (AIP, Melville, New York, 2003), pp. 267–272
7. M. Sadli, F. Bourson, M. Fanjeaux, S. Briaudeau, B. Rougié, G. Bonnier, in *Proceedings of TEMPMEKO 2004, 9th International Symposium on Temperature and Thermal Measurements in Industry*

- and Science*, ed. by D. Zvizdić, L.G. Bermanec, T. Veliki, T. Stašić (FSB/LPM, Zagreb, Croatia, 2004), pp. 611–616
8. K. Anhalt, J. Hartmann, D. Lowe, G. Machin, M. Sadli, Y. Yamada, P. Bloembergen, *Metrologia* **43**, S78–S83 (2006)
 9. G. Machin, P. Bloembergen, J. Hartmann, M. Sadli, Y. Yamada, in *Proceedings of TEMPMEKO 2007*. *Int. J. Thermophys.* **28**, 1976 (2007), doi:[10.1007/s10765-007-0250-7](https://doi.org/10.1007/s10765-007-0250-7)
 10. Y. Yamada, B. Khlevnoy, Y. Wang, T. Wang, K. Anhalt, *Metrologia* **43**, S140 (2006)
 11. M. Sadli, K. Anhalt, F. Bourson, S. Schiller, J. Hartmann, in *Proceedings of TEMPMEKO 2007*, *Int. J. Thermophys.*, doi:[10.1007/s10765-008-0479-9](https://doi.org/10.1007/s10765-008-0479-9)
 12. B. Khlevnoy, M. Sakharov, S. Ogarev, V. Sapritsky, Y. Yamada, K. Anhalt, in *Proceedings of TEMPMEKO 2007*, *Int. J. Thermophys.* **29**, 271 (2008), doi:[10.1007/s10765-007-0347-z](https://doi.org/10.1007/s10765-007-0347-z)
 13. S. Briaudeau, B. Rougié, M. Fanjeaux, M. Sadli, G. Bonnier, in *Proceedings of TEMPMEKO 2004, 9th International Symposium on Temperature and Thermal Measurements in Industry and Science*, ed. by D. Zvizdic (FSB/LPM, Zagreb, Croatia, 2004), pp. 119–125